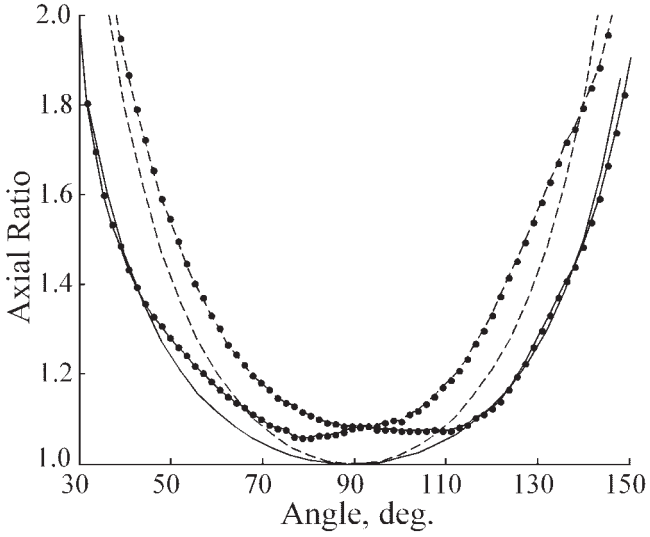

Figure 5 Axial polarization ratio versus angle θ of folded-wire X antenna with flat reflector for two radiation pattern cut planes: $\phi = 0°$ (numerical-solid line and measured-solid line with dots) and $\phi = 45°$ (numerical-dashed line and measured-dashed line with dots)

figure) is similar to the AR curve in $\phi = 0°$ plane. It is seen that in the peak gain direction $\theta = 90°$, where AR = 1 (or 0 dB) in theory, the measured value AR = 1.1 (or 0.8 dB) is quite close. Within the beamwidth region (or −3 dB-angular sector) of the gain radiation pattern AR is less than 1.41 or 3 dB, which is well within the customary requirements for medium-gain antennas with circular polarization [9].

4. CONCLUSIONS

In this article a folded-wire X antenna is introduced and applied for construction of a low-profile directive flat-reflector antenna. The two orthogonal input ports of the X antenna produce the same gain radiation patterns but different orthogonal polarizations. Both ports of the studied UHF X antenna model have equal input impedances of about 160 Ω at resonance. Because of its structural symmetry, the X antenna possesses very large inter-port and far-field cross-polar isolations. The single-port fed X antenna behaves like a half-wave dipole and the double-port fed X antenna acts as an array of two crossed dipoles.

The low-profile X antenna located in front of a flat reflector has a very simple feed circuit, where both ports are connected to two 50- Ω coaxial cables (loads) in balun-like manner. Compared with the standard reflector antenna with an active element (dipole, loop, and X antenna) located at a distance of 0.25–0.35 wavelengths, the low-profile reflector X antenna features about 2.5–3.0 dB higher gain, and thus, possesses an useful super-directivity. In addition, the reflector X antenna has much better input and cross-polar isolation compared with the similar low-profile array of two folded half-wave dipoles located in front of the same-size flat reflector.

Future applications of the folded-wire X antennas may include linear or circular polarization diversity RF/microwave earth or satellite communication and measurement systems, radars, etc.

ACKNOWLEDGMENTS

The authors acknowledge the financial support by the Chilean Conicyt Agency under the Bicentenario Project ATC-11/2004 and Fondecyt Project 1070742/2007.

REFERENCES

1. G.A. Lindberg, A shallow-cavity UHF crossed-slot antenna, IEEE Trans Antenna Propag 17 (1969), 558–563.
2. G.H. Brown, The 'turnstile' antenna, Electronics (1936), p. 15.
3. H. Kawakami, G. Sato, and R.W. Masters, Characteristics of TV transmitting batwing antennas, IEEE Trans Antenna Propag 32 (1984), 1318–1326.
4. A.G. Roederer, The crossed antenna: A new low-profile circularly polarized radiator, IEEE Trans Antenna Propag 38(1990), 704–710.
5. H.D. Hristov, Double-wire X-shape symmetrical antenna, Bulgarian Patent, 18 386, Class H 01 q 9/44, NPO, Sofia, 1968.
6. WIPL-D Pro, v. 5.1, 3D Electromagnetic Solver, WIPL-D d.o.o., 2004.
7. A. Kumar and H.D. Hristov, Microwave cavity antennas, Artech House, Inc., MA: Norwood, 1989.
8. J.D. Kraus and R.J. Marhefka, Antennas for all applications, 3rd ed., McGraw Hill, New York, NY, 2002.
9. R.C. Johnson, H. Jasik's Handbook, 3rd ed., Antenna Engineering Handbook, McGraw-Hill, New York, NY, 1993.

SMALL-SIZE PRINTED LOOP ANTENNA FOR PENTA-BAND THIN-PROFILE MOBILE PHONE APPLICATION

Kin-Lu Wong and Wei-Yu Chen
Department of Electrical Engineering, National Sun Yat-Sen University, Kaohsiung 80424, Taiwan; Corresponding author: chenwy@ema.ee.nsysu.edu.tw

Received 26 September 2008

ABSTRACT: *A planar printed loop antenna with a small area of 15 × 50 mm^2 and capable of covering all five operating bands of GSM850/900/1800/1900/UMTS for WWAN (wireless wide area network) operation in the thin-profile mobile phone is presented. The antenna is very suitable to be directly printed on the system circuit board of the mobile phone, making it easy to fabricate at low cost and generally showing no thickness above the circuit board; the latter is very attractive for thin-profile mobile phone applications. In addition, the proposed loop antenna is very suitable to be printed at the bottom position of the mobile phone; in this case the antenna meets the SAR (specific absorption rate) limit for practical applications.* © 2009 Wiley Periodicals, Inc.
Microwave Opt Technol Lett 51: 1512–1517, 2009; Published online in Wiley InterScience (www.interscience.wiley.com). DOI 10.1002/mop.24359

Key words: *internal mobile phone antennas; printed loop antennas; penta-band operation; printed antennas; WWAN antennas*

1. INTRODUCTION

Thin-profile mobile phones are recently becoming very attractive for mobile users on the market. For this application, the internal antennas to be embedded inside the mobile phone should be of very thin profile, in addition to occupying a small area on the system circuit board of the mobile phone. In addition, all five operating bands of GSM850/900/1800/1900/UMTS (824–894/890–960/1710–1880/1850–1990/1920–2170 MHz) for WWAN operation should also be covered. To meet the requirements, the internal antennas that can be directly printed on the system circuit board of the mobile phone are promising candidates. There are also several reported internal printed antennas capable of the desired penta-band operation [1–6]. These reported designs include the printed loop-type antenna [1], the printed slot antenna [2], the printed monopole slot antenna [3, 4], the printed PIFA (planar

inverted-F antenna) [5], and the printed monopole antenna with an external matching circuitry [6]; they all can be directly printed on the system circuit board of the mobile phone. The occupied board space is about 900 mm^2 [1, 2] or 600 mm^2 only [3–6] and generally shows no thickness above the circuit board, which is, hence, very attractive for thin-profile mobile phone applications.

In this study, we present another promising internal printed antenna capable of penta-band operation and also occupying a small area on the system circuit board of the mobile phone. The proposed design uses the printed loop structure, which has been known to be capable of resulting in small excited surface current distributions on the system circuit board of the mobile phone [7–18]. This behavior is expected to result in decreased user's hand effects on the radiation efficiency of the internal antenna [7]. This attractive property motivates the proposed loop antenna study in this article, which is believed to be the first printed loop antenna with a small occupied area (750 mm^2 in this study) and capable of penta-band operation that have been reported in the open literature.

In addition, it is proposed in this study that the printed loop antenna be mounted at the bottom position of the system circuit board of the mobile phone, adopting the technique that has been used in some available mobile phones on the market to achieve reduced SAR values. In this case, the SAR [19–21] results of the mobile phone with the proposed printed loop antenna in the five operating bands of GSM850/900/1800/1900/UMTS can all meet the limit of 1.6 W/kg for the 1-g head tissue or 2.0 W/kg for the 10-g head tissue [21]. Details of the proposed antenna are described, and results of the fabricated prototype, including the SAR analysis, are presented and discussed.

2. PROPOSED PRINTED LOOP ANTENNA

Figure 1(a) shows the geometry of the proposed printed loop antenna at the bottom position of the system circuit board of the mobile phone, and dimensions of the printed metal pattern of the antenna are given in Figure 1(b). In the study, a 0.8-mm thick FR4 substrate of relative permittivity 4.4 and size 115 × 50 mm^2 considered as the system circuit board of the practical mobile phone on the market is used. On the back side of the FR4 substrate, there is a printed ground plane of size 100 × 50 mm^2, leaving a no-ground portion of 15 × 50 mm^2 at the bottom position of the circuit board. At the no-ground portion, the proposed loop antenna is printed.

The proposed loop antenna comprises an outer loop strip and two inner strips therein. The outer loop strip is generally of a narrow width 0.5 mm and provides a resonant loop path of about 150 mm to generate a 0.5λ loop mode at about 900 MHz (denoted as mode 1 here) and a 1.0λ loop mode at about 1850 MHz (denoted as mode 2) for the proposed antenna. Note that there are two meandered sections along the outer loop strip to achieve a lengthened resonant loop path in the small no-ground portion. One end (point A) of the outer loop strip is the feeding point of the antenna, whereas the other end (point B) is grounded to the top edge of the system ground plane through a via hole in the FR4 substrate. To test the antenna in the experiment, a 50-Ω microstrip feedline is printed on the front side of the FR4 substrate and connected to point A for feeding the antenna.

Inside the outer loop strip, two inner strips are embedded, which result in two additional resonant loop paths in the proposed design. The longer one (inner strip 1) is connected to the outer loop strip at a position close to the grounding point (point B) and is extended to the other side of the outer loop strip, with its open end (point C) pointing toward the loop strip at which the strip width is widened to 1 mm for better coupling between the inner strip 1 and

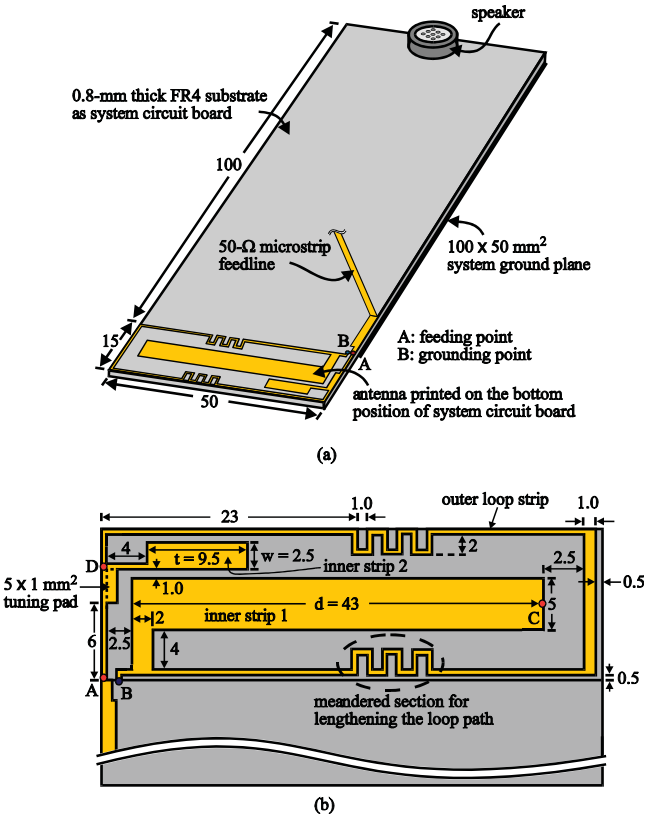

Figure 1 (a) Geometry of the proposed loop antenna printed at the bottom position of the system circuit board of the mobile phone. (b) Dimensions of the metal pattern of the antenna. [Color figure can be viewed in the online issue, which is available at www.interscience.wiley.com]

the loop strip. In this case, a second resonant loop path of length about 138 mm is generated, which starts from point A, follows along the loop strip, capacitively couples to the inner strip 1 at the widened loop section and then ends at point B. This resonant path can support a 0.5λ loop mode at frequencies close to 900 MHz (denoted as mode 3 here), which incorporates mode 1 supported by the outer loop strip to form a wide lower band covering GSM850/900 operation.

For the inner strip 2, it is connected to the front section of the outer loop strip at point D and supports a third resonant path of length about 48 mm, which starts from points A to D, enters into the inner strip 2, then capacitively couples to inner strip 1 and ends at point B. This resonant path results in the excitation of a 0.5λ loop mode at about 2100 MHz (denoted as Mode 4 here). Mode 4 is adjusted to occur at frequencies adjacent to Mode 2 supported by the outer loop strip. Modes 4 and 2 are formed into a wide upper band covering GSM1800/1900/UMTS operation.

Also note that there is a small tuning pad (5 × 1 mm^2) added at point D to the outer loop strip, which is used for fine-tuning the impedance matching of the excited resonant modes to form the desired wide lower and upper bands. This tuning-pad effect on improving the impedance matching of the loop antenna is similar to the results observed in [16]. In sum, there are three resonant loop paths provided in the proposed antenna, which support four resonant modes to form into two wide operating bands centered at about 900 and 2000 MHz for the desired penta-band operation. Detailed excited surface current distributions on the proposed antenna for the three resonant loop paths are presented and discussed in Figure 5 in the next section.

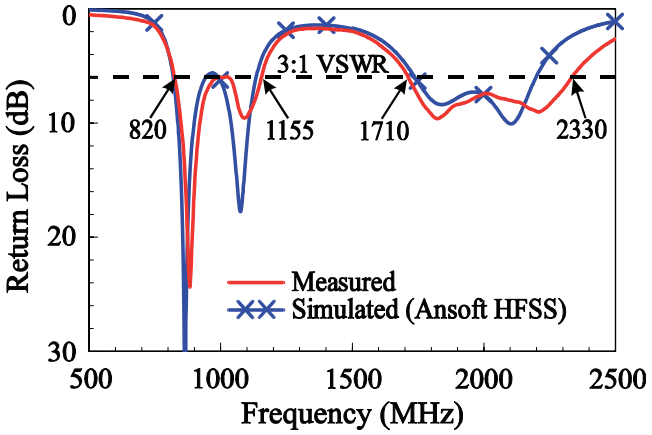

Figure 2 Measured and simulated return loss of the proposed antenna. [Color figure can be viewed in the online issue, which is available at www.interscience.wiley.com]

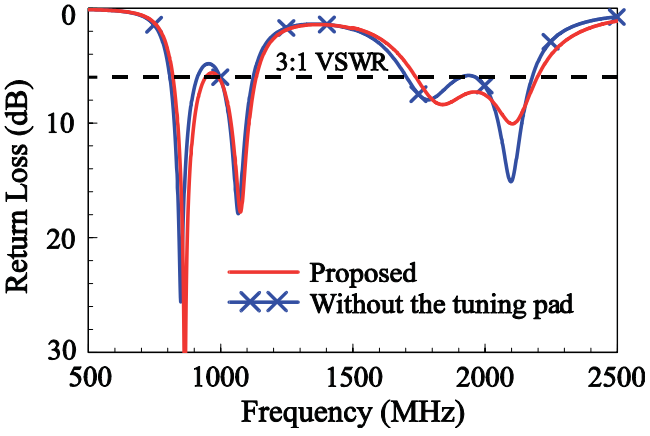

Figure 4 Simulated return loss for the proposed antenna and the case without the tuning pad at point D. [Color figure can be viewed in the online issue, which is available at www.interscience.wiley.com]

3. RESULTS AND DISCUSSION

The proposed antenna was fabricated and tested. Figure 2 shows the measured and simulated return loss. Agreement between the measured data and the simulated results obtained using Ansoft HFSS [22] is seen. Two wide operating bands centered at about 980 and 2000 MHz are obtained. The lower band is formed by two resonant modes, which are the Mode 1 and Mode 3 as described in Section 2, and shows a large measured bandwidth of 355 MHz (820–1155 MHz) to easily cover GSM850/900 operation. The upper band is also formed by two resonant modes (Modes 2 and 4 described in Section 2), and a large measured bandwidth of 620 MHz (1710–2330 MHz) is achieved for covering GSM1800/1900/UMTS operation. Five operating bands for WWAN operation are, hence, covered by the proposed printed loop antenna.

Figure 3 shows the simulated return loss for the proposed antenna and the case without the inner strip 2. It is clearly seen that with the presence of the inner strip 2, an additional resonant mode at about 2100 MHz is generated, which incorporates with the resonant mode (Mode 2 described in Section 2) supported by the outer loop strip to form the desired upper band for GSM1800/1900/UMTS operation.

Figure 4 presents the simulated return loss for the proposed antenna and the case without the tuning pad at point D. When the tuning pad is added, the impedance matching at adjacent frequencies between the two resonant modes in both the lower and upper bands is improved, leading to good coverage of the GSM850/900 and GSM1800/1900/UMTS bands for the proposed antenna.

To study the three resonant loop paths provided in this design, the excited surface current distributions on the proposed antenna and the system ground plane at about the central frequencies (865, 1100, 1850, and 2100 MHz) of the four excited resonant modes are presented in Figure 5(a). Also, the corresponding vector current distributions on the proposed antenna are shown in Figure 5(b). At 865, 1100, and 2100 MHz, there is one current null observed in the three resonant loop paths supported by the proposed antenna as

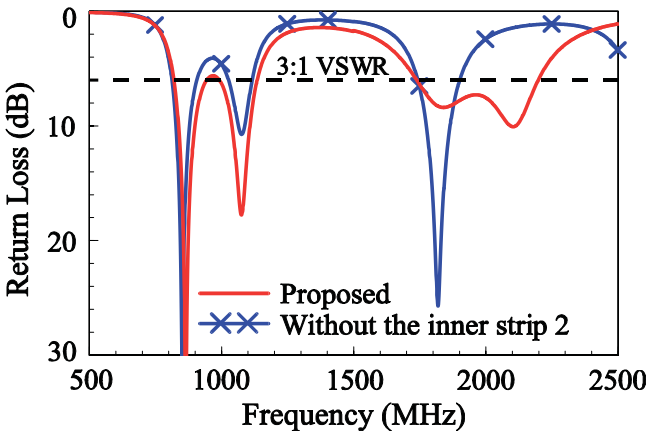

Figure 3 Simulated return loss for the proposed antenna and the case without the inner strip 2. [Color figure can be viewed in the online issue, which is available at www.interscience.wiley.com]

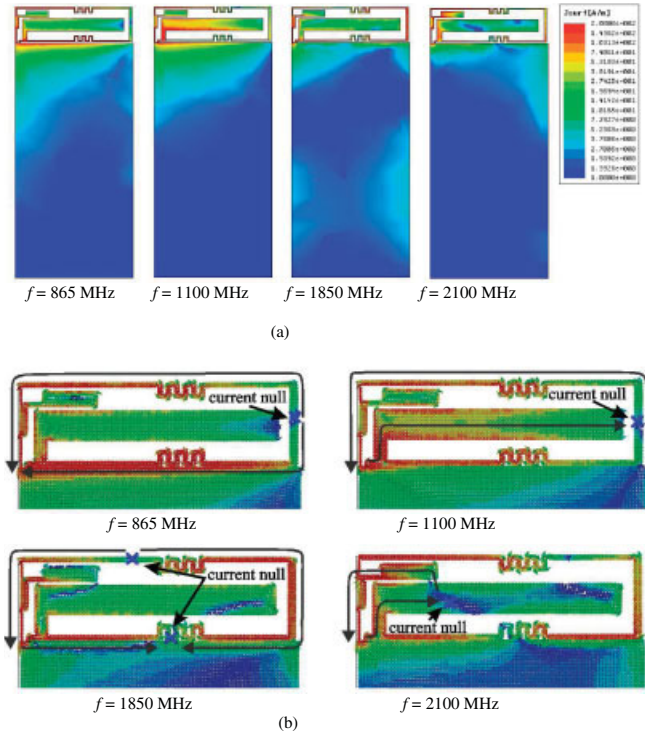

Figure 5 (a) Simulated excited surface current distributions on the proposed antenna and the system ground plane. (b) Vector current distributions on the proposed antenna. [Color figure can be viewed in the online issue, which is available at www.interscience.wiley.com]

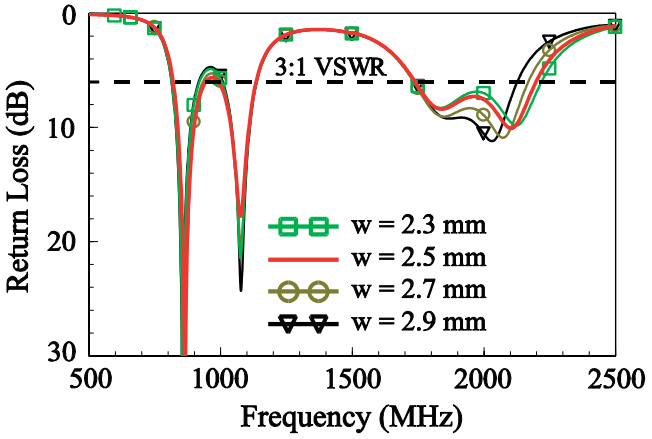

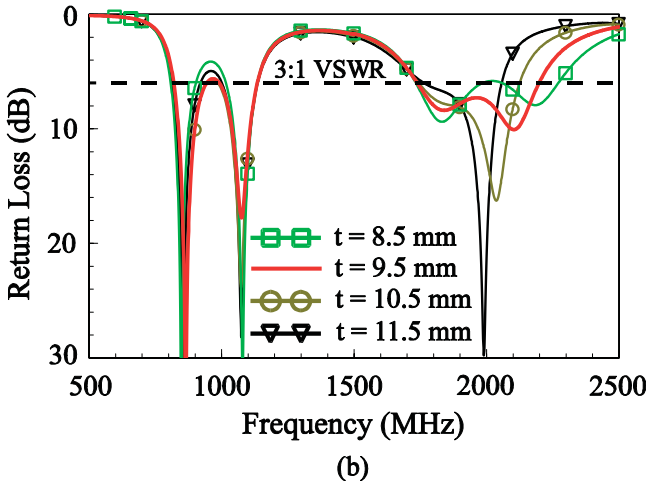

Figure 6 Simulated return loss as a function of (a) the width w and (b) the length t in the inner strip 2. Other dimensions are the same as given in Figure 1. [Color figure can be viewed in the online issue, which is available at www.interscience.wiley.com]

described in Section 2. That is, the three resonant modes (Modes 1, 3, and 4 described in Section 2) can be regarded as the 0.5λ loop modes supported by the three resonant loop paths. At 1850 MHz, two current nulls in the resonant loop path supported by the outer loop strip are seen; this resonant loop (Mode 2) can, hence, be regarded as 1.0λ loop mode supported by the outer loop strip.

Figure 6 shows the simulated return loss as a function of the width w and the length t in the inner strip 2; other dimensions are the same as given in Figure 1. Results for the width w varied from 2.3 to 2.9 mm are shown in Figure 6(a), and large effects on the impedance matching of the resonant mode at about 2100 MHz (Mode 4 described in Section 2) are seen. Figure 6(b) shows the results for the length t varied from 8.5 to 11.5 mm, and large effects on the resonant frequencies of Mode 4 are observed. When the length t increases, the resonant frequency of Mode 4 is shifted to lower frequencies. These results indicate that by adjusting the width w and length t in the inner strip 2, excitation of Mode 4 can be controlled, which agrees with the discussion in Section 2.

Effects of the inner strip 1 are analyzed in Figure 7, in which results of the simulated return loss as a function of the length d in the inner strip 1 are shown. In this case, significant effects on the resonant mode at about 1100 MHz (Mode 3 described in Section

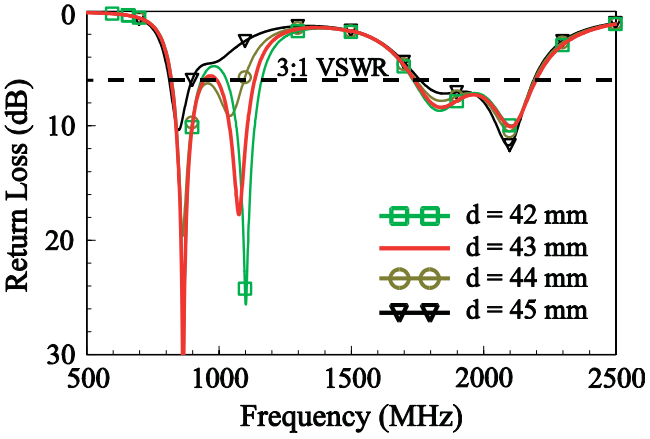

Figure 7 Simulated return loss as a function of the length d in the inner strip 1. Other dimensions are the same as given in Figure 1. [Color figure can be viewed in the online issue, which is available at www.interscience.wiley.com]

2) are seen. Results indicate that a proper selection of the length d is required for successful excitation of Mode 2 to achieve a wide lower band for the proposed antenna.

Radiation characteristics of the proposed antenna were also studied. Figure 8 plots the measured and simulated three-dimen-

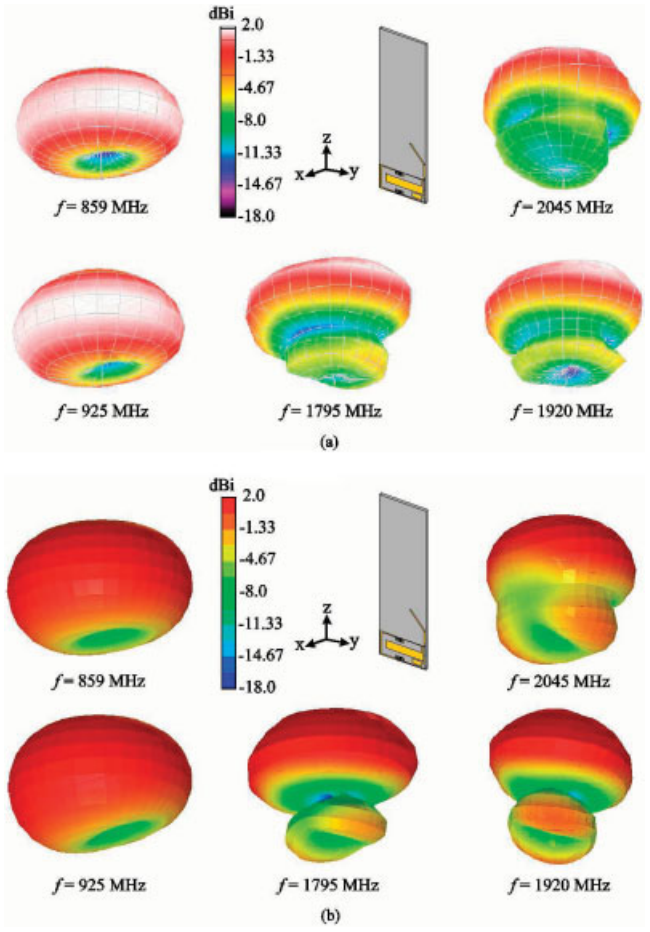

Figure 8 (a) Measured and (b) simulated 3-D total power radiation patterns at 859, 925, 1795, 1920, and 2045 MHz for the proposed antenna. [Color figure can be viewed in the online issue, which is available at www.interscience.wiley.com]

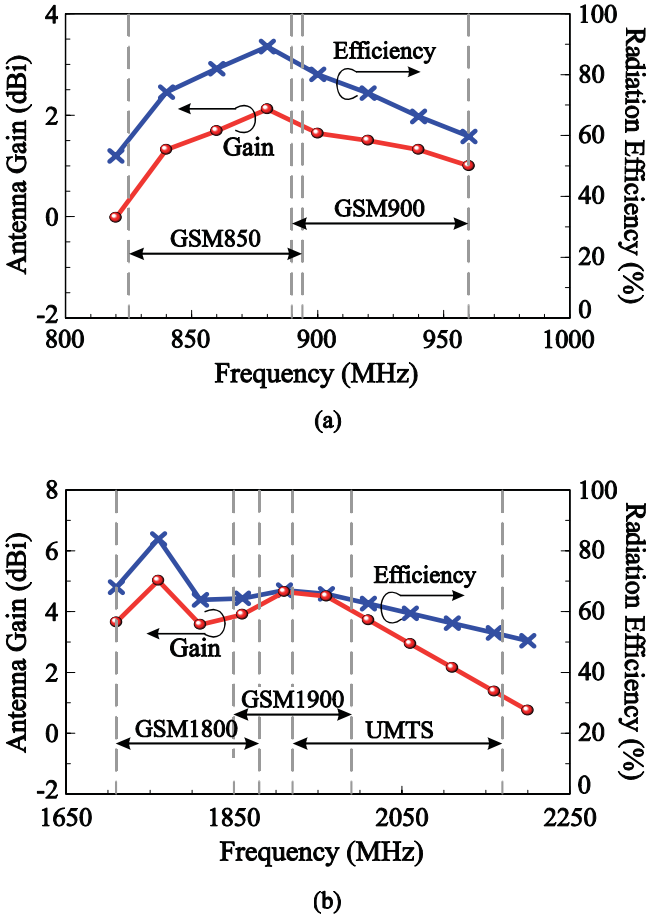

Figure 9 Measured antenna gain and radiation efficiency for the proposed antenna. (a) Lower band for GSM850/900 operation. (b) Upper band for GSM1800/1900/UMTS operation. [Color figure can be viewed in the online issue, which is available at www.interscience.wiley.com]

sional (3-D) total power radiation patterns at 859, 925, 1795, 1920, and 2045 MHz (central frequencies of the five operating bands). Agreement between the measurement and simulation is obtained. Monopole-like radiation patterns are seen at 859 and 925 MHz, which are similar to the corresponding radiation patterns for the traditional internal mobile phone antennas [23]. This is because the system ground plane of the mobile phone is a major radiator for operating in the 900 MHz band [24]. For higher frequencies at 1795, 1920, and 2045 MHz, more variations in the radiation patterns are seen. This characteristic is owing to the increased groundplane length in term of the operating wavelength, thus making the excited surface currents in the ground plane vary more rapidly for operating in the antenna's upper band than in the lower band. This in turn results in more variations in the radiation patterns observed for higher frequencies.

Figure 9 shows the measured antenna gain and radiation efficiency for the proposed antenna. In Figure 9(a), results for the antenna's lower band are shown. The measured antenna gain is varied from about 0.3 to 2.0 dBi, while the radiation efficiency is better than 58%. Results for the antenna's upper band are given in Figure 9(b). The antenna gain is varied from about 1.2 to 5.0 dBi, and the radiation efficiency is in the range of 52–83%.

The SAR results of the proposed antenna are also analyzed. Table 1 lists the simulated SAR in 1-g and 10-g head tissues obtained from SEMCAD [25] for two cases of the antenna's feeding point A facing downward (Case 1) and upward (Case 2) with the presence of the phantom head. The simulation model and the corresponding simulated SAR results at 859, 925, 1795, 1920, and 2045 MHz for Cases 1 and 2 are also shown in Figure 10. The SAR results are tested using 24 dBm (2 W continuous power in 1/8 time slot) at 859 and 925 MHz and 21 dBm (1 W continuous power in 1/8 time slot) at 1795, 1920, and 2045 MHz. Also, the system circuit board is spaced 5 mm to the phantom ear for considering the thickness of the mobile phone casing. For both cases, the SAR results varies slightly, and they all meet the limit of 1.6 W/kg for the 1-g head tissue or 2.0 W/kg for the 10-g head tissue [26]. That is, the proposed antenna placed at the bottom position of the mobile phone is promising for practical applications.

Also note that for the SAR distributions shown in Figure 10, the square marks in the figure represent the local SAR maximum. For lower frequencies at 859 and 925 MHz, there is one local SAR maximum located at about the center of the system ground plane for Cases 1 and 2. On the other hand, two local SAR maxima are seen for higher frequencies at 1795, 1920, and 2045 MHz. The two local SAR maxima indicate that the radiation energy is more uniformly distributed for higher frequencies than for lower frequencies. This characteristic is similar to that observed in [20].

4. CONCLUSION

A penta-band loop antenna suitable to be directly printed on the system circuit board of the mobile phone with a small occupied area of 15 × 50 mm^2 has been proposed and studied. The proposed antenna is easy to fabricate at low cost and capable of generating two wide operating bands for covering GSM850/900 and GSM1800/1900/UMTS operation. The antenna is espe-

TABLE 1 Simulated SAR in 1-g and 10-g Head Tissues Obtained from SEMCAD [25] for Two Cases of the Antenna's Feeding Point A Facing Downward (Case 1) and Upward (Case 2) with the Presence of the Phantom Head

	SAR_{1g} (W/kg)				
Antenna Orientation	859 MHz	925 MHz	1795 MHz	1920 MHz	2045 MHz
Point A facing downward	1.58	1.57	0.92	0.73	0.55
(Return loss)	(13.3 dB)	(9.0 dB)	(8.3 dB)	(6.9 dB)	(9.2 dB)
Point A facing upward	1.48	1.45	0.92	0.78	0.72
(Return loss)	(13.4 dB)	(8.8 dB)	(9.3 dB)	(7.6 dB)	(10.5 dB)
Point A facing downward	1.15	1.13	0.58	0.45	0.34
(Return loss)	(13.3 dB)	(9.0 dB)	(8.3 dB)	(6.9 dB)	(9.2 dB)
Point A facing upward	1.09	1.07	0.59	0.50	0.45
(Return loss)	(13.4 dB)	(8.8 dB)	(9.3 dB)	(7.6 dB)	(10.5 dB)

The return loss indicates the impedance matching level at each frequency for evaluating the SAR.

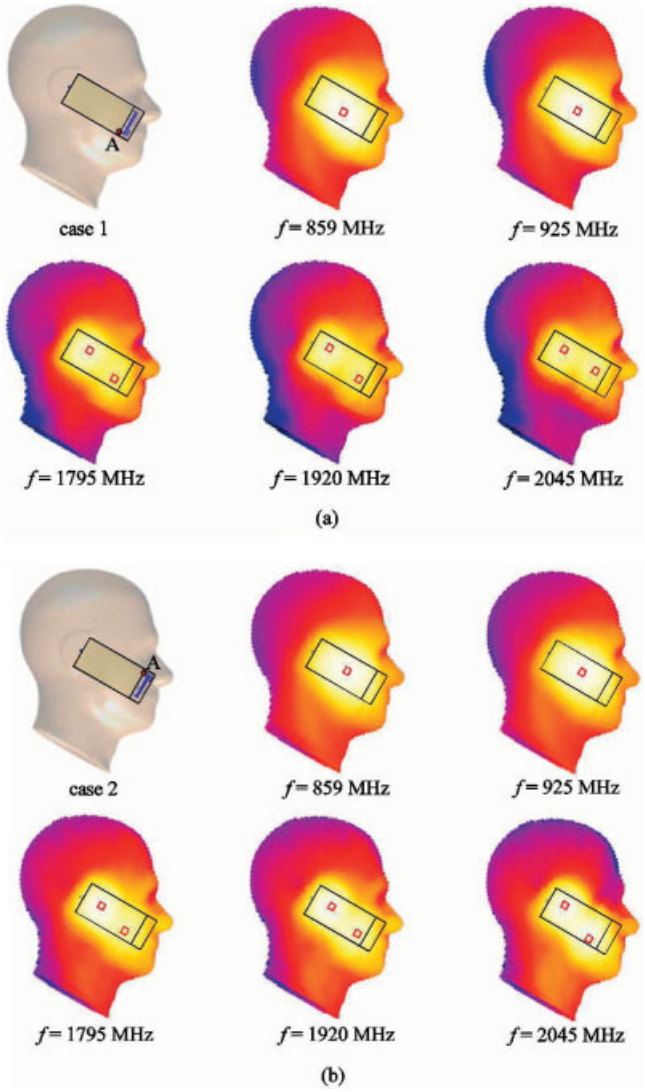

Figure 10 Simulated SAR distributions in 1-g head tissue at 859, 925, 1795, 1920, and 2045 MHz. (a) The case with antenna's feeding point A facing downward (Case 1). (b) The case with antenna's feeding point A facing upward (Case 2). [Color figure can be viewed in the online issue, which is available at www.interscience.wiley.com]

cially suited to be placed at the bottom position of the thin-profile mobile phone for practical applications. Good radiation characteristics for frequencies over the five operating bands have been obtained. The SAR results of the proposed antenna have also been found to meet the limit of 1.6 W/kg for the 1-g head tissue or 2.0 W/kg for the 10-g head tissue, indicating the proposed antenna is very promising for penta-band thin-profile mobile phone applications.

REFERENCES

1. W.Y. Li and K.L. Wong, Internal printed loop-type mobile phone antenna for penta-band operation, Microwave Opt Technol Lett 49 (2007), 2595–2599.
2. C.H. Wu and K.L. Wong, Hexa-band internal printed slot antenna for mobile phone application, Microwave Opt Technol Lett 50 (2008), 35–38.
3. C.I. Lin and K.L. Wong, Printed monopole slot antenna for internal multiband mobile phone antenna, IEEE Trans Antennas Propag 55 (2007), 3690–3697.
4. C.I. Lin and K.L. Wong, Printed monopole slot antenna for penta-band operation in the folder-type mobile phone, Microwave Opt Technol Lett 50 (2008), 2237–2241.
5. K.L. Wong and C.H. Huang, Printed PIFA with a coplanar coupling feed for penta-band operation in the mobile phone, Microwave Opt Technol Lett 50 (2008), 3181–3186.
6. K.L. Wong and T.W. Kang, GSM850/900/1800/1900/UMTS printed monopole antenna for mobile phone application, Microwave Opt Technol Lett 50 (2008), 3192–3198.
7. Y.W. Chi and K.L. Wong, Internal compact dual-band printed loop antenna for mobile phone application, IEEE Trans Antennas Propag 55 (2007), 1457–1462.
8. K.D. Katsibas, C.A. Balanis, P.A. Tirkas, and C.R. Birtcher, Folded loop antenna for mobile hand-held units, IEEE Trans Antennas Propag 46 (1998), 260–266.
9. H. Morishita, H. Furuuchi, and K. Fujimoto, Characteristics of a balance-fed loop antenna system for handsetsin the vicinity of human head or hand, IEEE Antennas Propag Soc Int Symp Dig 4 (2000), 2254–2257.
10. S. Hayashida, T. Tanaka, H. Morishita, Y. Koyanagi, and K. Fujimoto, Built-in monopole antenna for handsets, Electron Lett 40 (2004), 1514–1516.
11. C.C. Chiau, X. Chen, and C.G. Parini, A miniature dielectric-loaded folded half-loop antenna and ground plane effects, IEEE Antennas Wireless Propag 4 (2005), 459–462.
12. B.K. Yu, B. Jung, H.J. Lee, F.J. Harackiewicz, and B. Lee, A folded and bent internal loop antenna for GSM/DCS/PCS operation of mobile handset applications, Microwave Opt Technol Lett 48 (2006), 463–467.
13. B. Jung, H. Rhyu, Y.J. Lee, F.J. Harackiewicz, M.J. Park, and B. Lee, Internal folded loop antenna with tuning notches for GSM/GPS/DCS/PCS mobile handset applications, Microwave Opt Technol Lett 48 (2006), 1501–1504.
14. C.I. Lin and K.L. Wong, Internal meandered loop antenna for GSM/DCS/PCS multiband operation in a mobile phone with the user's hand, Microwave Opt Technol Lett 49 (2007), 759–s765.
15. W.Y. Li and K.L. Wong, Surface-mount loop antenna for AMPS/GSM/DCS/PCS operation in the PDA phone, Microwave Opt Technol Lett 49 (2007), 2250–2254.
16. K.L. Wong and C.H. Huang, Printed loop antenna with a perpendicular feed for penta-band mobile phone application, IEEE Trans Antennas Propag 56 (2008), 2138–2141.
17. Y.W. Chi and K.L. Wong, Half-wavelength loop strip fed by a printed monopole for penta-band mobile phone antenna, Microwave Opt Technol Lett 50 (2008), 2549–2554.
18. Y.W. Chi and K.L. Wong, Compact multiband folded loop chip antenna for small-size mobile phone, IEEE Trans Antennas Propag, in press.
19. O. Kivekas, J. Ollikainen, T. Lehtiniemi, and P. Vainikainen, Bandwidth, SAR, and efficiency of internal mobile phone antennas, IEEE Trans Electromagn Compatibility 46 (2004), 71–86.
20. Z. Li and Y. Rahmat-Samii, Optimization of PIFA-IFA combination in handset antenna design, IEEE Trans Antennas Propag 53 (2005), 1770–1777.
21. O. Sotoudeh and T. Wittig, Electromagnetic simulation of mobile phone antenna performance, Microwave J 51 (2008), 78–92.
22. Ansoft Corporation, Available at http://www.ansoft.com/products/hf/hfss/, Ansoft Corporation HFSS, Pittsburg, PA.
23. K.L. Wong, Planar Antennas for wireless communications, Wiley, New York, 2003.
24. P. Vainikainen, J. Ollikainen, O. Kivekas, and I. Kelander, Resonator-based analysis of the combination of mobile handset antenna and chassis, IEEE Trans Antennas Propag 50 (2002), 1433–1444.
25. Schmid & Partner Engineering AG (SPEAG), Available at http://www.semcad.com, SPEAG SEMCAD.
26. J.C. Lin, Specific absorption rates induced in head tissues by microwave radiation from cell phones, Microwave 44 (2001), 22–25.